Progress In Electromagnetics Research Letters, Vol. 91, 145–152, 2020

Low Cost Substrate Based Compact Antennas for 4G/5G Side-Edge Panel Smartphone Applications

Issmat S. Masoodi, Insha Ishteyaq, Khalid Muzaffar*, and Muhammad I. Magray

Abstract—The integrated design of 4G LTE and mmWave 5G antennas based on a low cost substrate is proposed for mobile terminals. The 4G LTE antenna is designed along with the millimeter wave 5G antenna element, and this integrated module is mounted orthogonally to cater for smartphone applications. The 4G LTE module consists of two orthogonally placed compact asymmetric coplanar strip (ACS) fed antennas which caters to LTE1900, LTE2300, and LTE2500 bands. ACS-fed antennas operate from 1.8 to 2.7 GHz with a reasonable gain ranging between 1.5 and 2.9 dBi. The mmWave 5G antenna module comprises two compact Vivaldi antennas with wideband operational bandwidth ranging from 23 to 39 GHz. Each mmWave 5G antenna attains 1-dB gain bandwidth of 47.6% indicating high radiation bandwidth across the operating frequency band. Orthogonal pattern diversity is achieved for the usage of smartphone in both portrait and landscape modes. The whole antenna architecture is accommodated to the panel of height 6 mm inside a fabricated three dimensional mobile phone case. Simulated and measured results are presented with technical justification.

1. INTRODUCTION

Communication engineers and hardware specialists across academia and industry believe that the future cellular communication systems would need to cater to high data rates which in turn translates to higher carrier frequencies than the existing ones [1]. The now famous testing campaign led by Prof. Rappaport is a testimony to the feasibility of millimeter wave frequencies, as carrier frequency for cellular communication system. The primary issue with using carrier frequencies beyond 20 GHz is the inherent free space path loss [2], which could be mitigated using high gain antennas on both the mobile device and access point or base station as demonstrated in [1]. It is well known that technology transition would happen in a sequential manner which provokes hardware engineers to design and deploy transceiver radio systems which are backward compatible as well. In other words, future millimeter wave 5G hardware would coexist with the older 4G radios. Hence, co-design of 4G and 5G antennas is the theme of this paper. The antenna to be integrated in a mobile device has several requirements such as electrically compact and low specific absorption rate for 4G antennas. But the antennas operational at 28 GHz must have high gain with low physical footprint. Even though several articles on co-design of 4G and 5G have been published [3–7], the edge panel integration for future mobile phones would not be feasible for these reported designs. Hence, a highly compact 4G LTE Multiple-Input Multiple-Output (MIMO) antenna integrated with a wideband high gain millimeter wave 5G MIMO antenna is proposed with detailed simulated and measured results.

2. LOW COST SUBSTRATE BASED 4G LTE AND MMWAVE 5G MIMO ANTENNA DESIGNS

The proposed antenna architecture consists of integrated 4G LTE and mmWave 5G antennas designed on a 20-mil thick polycarbonate substrate having dielectric constant (ε_r) of 2.9 and loss tangent of

Received 10 April 2020, Accepted 27 May 2020, Scheduled 8 June 2020

* Corresponding author: Khalid Muzaffar (khalid.muzaffar@islamicuniversity.edu.in).

The authors are with the Department of Electronics and Communication Engineering, Islamic University of Science & Technology, Awantipora, J&K, India.

0.01. All antenna designs and full wave simulations are performed in Computer Simulation Technology (CST) Microwave Studio. Polycarbonate substrate is chosen for its low cost and flexibility to obtain corner bending. For decreasing cross polarization in the end-fire, a thin substrate is chosen. Regarding the fabrication of proposed 4G LTE and mmWave 5G antennas, a polycarbonate substrate of desired dimensions is first pasted by copper tape of thickness 80 µm followed by industry standard chemical etching process applied on both sides of the substrate.

2.1. Design of 4G LTE Antenna

Schematics of the proposed co-designed 4G LTE and mmWave 5G antenna are depicted in Figs. 1(a) and (b) with top and bottom views, respectively. The proposed 4G LTE antenna section of the module consists of an ACS-fed antenna with a stepped radiator for achieving larger impedance bandwidth [8]. Since SMA connector would not be suitable for measurement purposes due to improper soldering contact between the launch pin and trace of ACS-fed 4G LTE antenna, a high frequency end-launch connector is used. The polycarbonate substrate is extended on both sides of feed line for mounting an industry standard 2.92 mm bulky end-launch connector. The proposed 4G LTE section of the antenna is fed by a 5 Ω ACS feedline, which is designed according to standard calculations with signal strip width of 1.5 mm, and the gap between signal trace and coplanar ground plane is 0.3 mm [9]. The operating frequency bandwidth of 4G LTE antenna is adjusted depending upon the number and length of steps inserted in the radiator. The proposed 4G LTE antenna is compact with dimension of $0.03\lambda \times 0.26\lambda \times 0.003\lambda$ at 1.8 GHz. The proposed integrated 4G LTE and mmWave 5G antenna is fabricated, and a photograph is shown in Fig. 2.

Measured results of the proposed antenna are obtained using Agilent PNA E8364C. The simulated and measured input reflection coefficients of the proposed ACS-fed 4G LTE antenna are depicted in Fig. 3(a). The proposed antenna operates from 1.8 to 2.7 GHz with fractional bandwidth of 40%. The

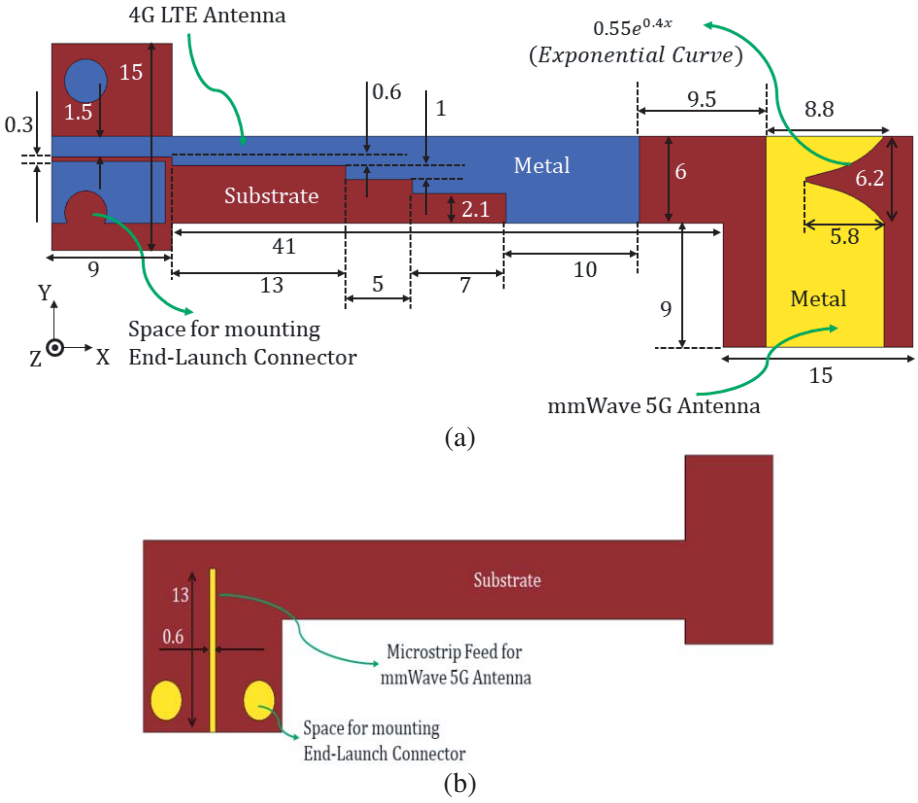

Figure 1. Schematics of the low cost substrate based co-designed 4G LTE and mmWave 5G module (a) top plane and (b) bottom plane (All dimensions are in mm).

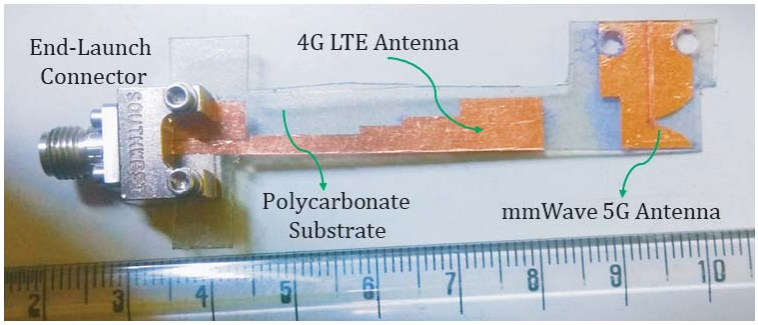

Figure 2. Photograph of the fabricated co-designed 4G LTE and mmWave 5G antenna.

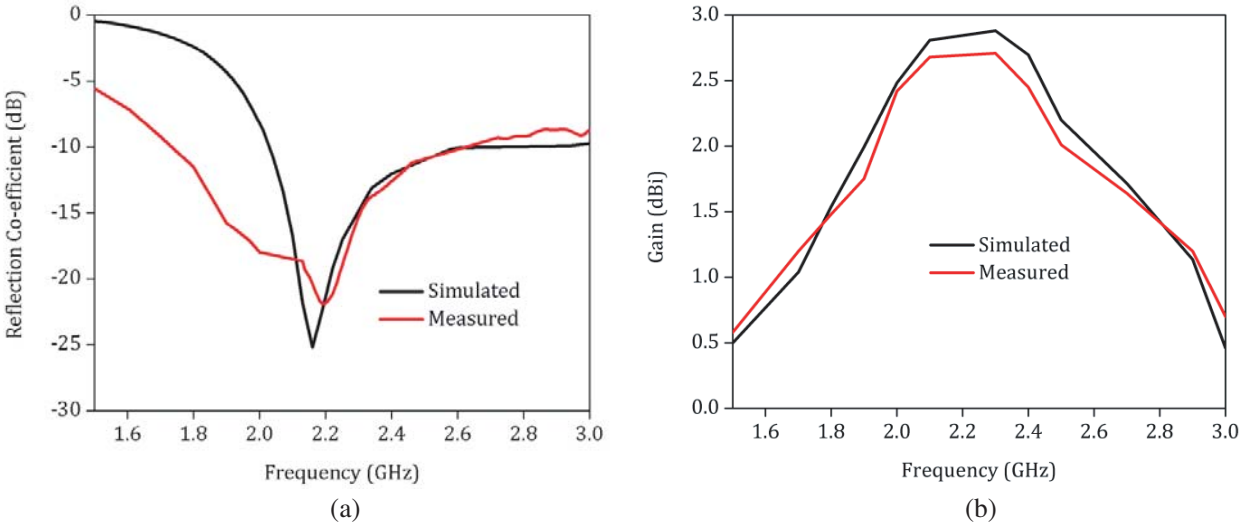

Figure 3. (a) Input reflection co-efficient and (b) gain plot of the proposed 4G LTE antenna.

proposed antenna is wideband covering various LTE bands like LTE1900 (1880-1900 MHz), LTE2300 (2300–2400 MHz), and LTE2500 (2500–2690 MHz). Discrepancies may be attributed to fabrication tolerances, solder-less transition from end-launch connector to ACS feedline, and port impedance variation from 50 Ω of the end-launch connector used for measurement purposes.

The proposed antenna attains broadside reasonable gain ranging from 1.5 to 2.9 dBi for the available electrical size as illustrated in Fig. 3(b). Simulated and measured radiation patterns in XZ-plane (E-plane) are illustrated in Fig. 4. The proposed antenna achieves dipole-like radiation patterns in E-plane. Disparity between simulated and measured radiation patterns could be attributed to poor absorptivity of indirect radiations inside an anechoic chamber. In addition, unpredicted radiations generated by the strayed currents induced in bulky end-launch connector might be the reason for the deviation between simulated and measured data.

2.2. Design of mmWave 5G Antenna

A compact electrically small Vivaldi antenna is designed on a low cost polycarbonate substrate for mmWave 5G mobile applications. Schematics of the mmWave 5G end-fire antenna integrated with 4G LTE antenna are depicted in Fig. 1. The proposed mmWave 5G antenna has the compact dimensions of $0.56\lambda \times 0.82\lambda \times 0.046\lambda$ at 28 GHz suitable for panel integration in commercial smartphones. The proposed design consists of a 50 Ω microstrip line that feeds the balun of antenna optimized for better impedance matching. The radiation curve of proposed Vivaldi antenna is an exponential function as

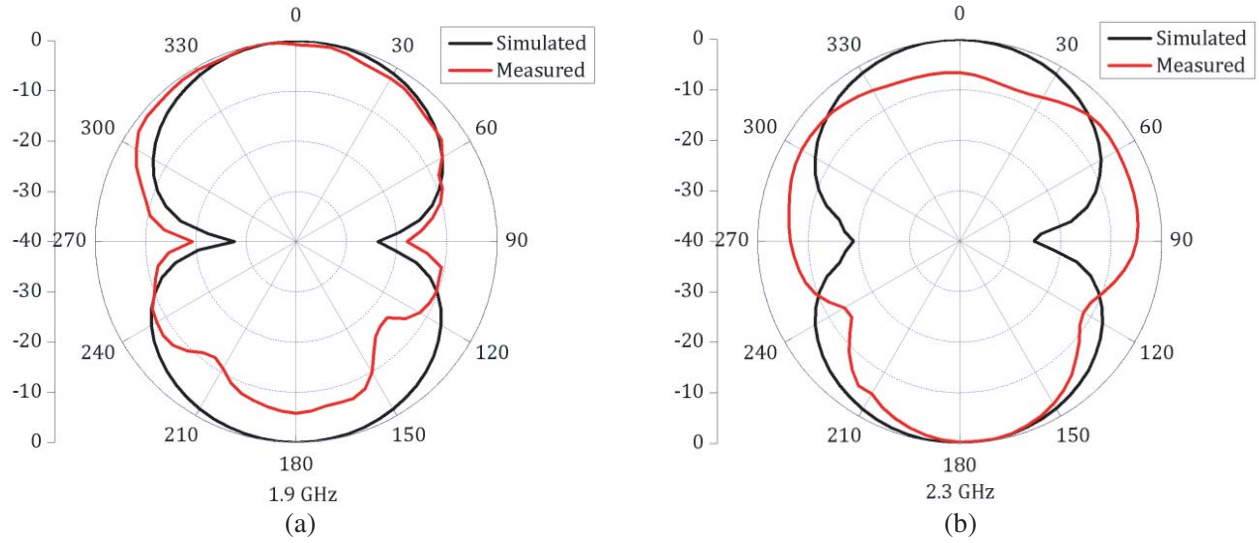

Figure 4. Radiation patterns in XZ-plane for proposed 4G LTE antenna.

described below [10]:

$$y = ae^{bx}, \tag{1}$$

where "a" is the distance from the center of slot-line to either of the exponential curve of Vivaldi antenna, i.e., half of the slot width of antenna; "b" is the rate of tapering; and "x" and "y" are the independent and dependent variables, respectively. For the proposed antenna, the values of "a" and "b" are 0.55 and 0.4 respectively as depicted in Fig. 1.

Separation of 0.9λ is chosen between the feeding plane of Vivaldi antenna and radiating aperture in order to avoid grounding contact and blockage of radiation with the industry standard 2.92 mm end-launch connector. Since the maximum radiating aperture for the proposed mmWave 5G antenna is around 0.5λ, traveling waves move through the metallic tapers and uncouple after half-wavelength separation is reached thereby producing end-fire radiation [11].

Simulated and measured input reflection coefficients for the proposed antenna are shown in Fig. 5(a). The proposed mmWave 5G Vivaldi antenna is wideband operating from 23 to 39 GHz

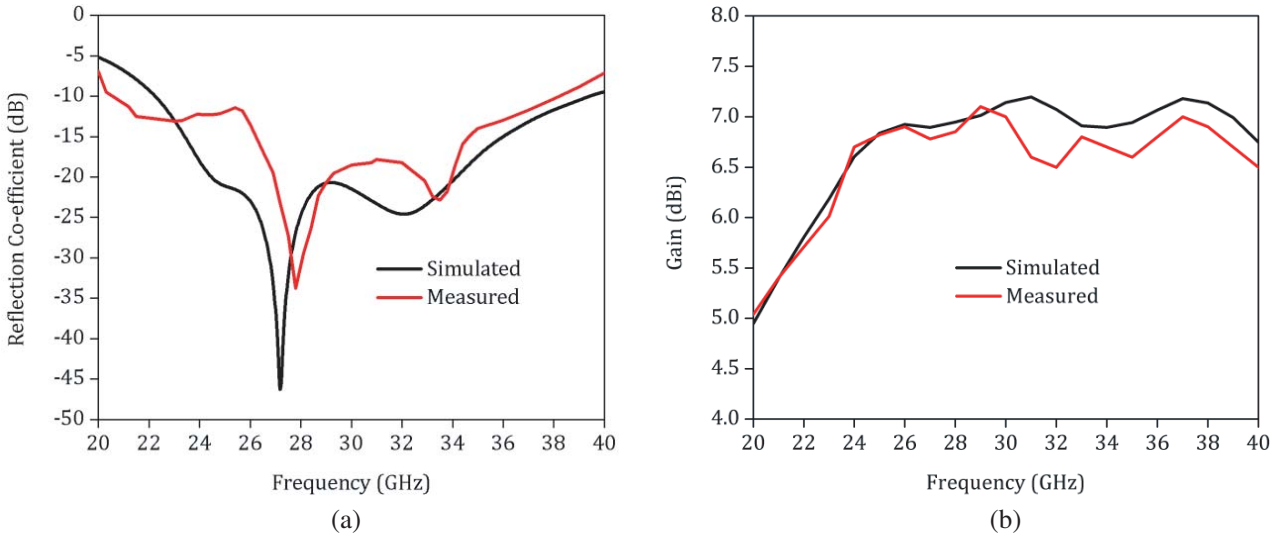

Figure 5. (a) Input reflection co-efficient and (b) gain plots of the proposed 4G LTE antenna.

with fractional bandwidth of 51.6%. Microstrip to slot-line transition is optimized for achieving larger impedance bandwidth. Discrepancies could be ascribed to fabrication tolerances and characteristic impedance variation from 50 Ω of end-launch connector. In addition to this, end-launch connector was not modelled in simulations, therefore could be the reason behind disparity between simulated and measured data.

High end-fire gain ranging from 6 to 7.2 dBi is attained for the available aperture as depicted in Fig. 5(b). It must be noted that the compact antenna designed for 5G application occupies an effective aperture of 6.2 mm (which is compliant with the panel dimension of most of the commercial smartphones) and 5.8 mm as observed in Fig. 1(a). Translating the same physical dimensions electrically, this is $0.58\lambda \times 0.54\lambda$ at 28 GHz. Typically, travelling wave antennas are designed with electrically large apertures of at least 1λ, which in turn would yield a radiation pattern with high pattern integrity and high gain [12–15]. However, in strong contrast to conventional Vivaldi based designs, the proposed traveling wave antenna is electrically compact which leads to lower gain due to reduced physical aperture. The patterns would be useful post integration in an actual mobile terminal as individual elements are fired up for portrait and landscape modes of operation hence avoiding the necessity of exorbitantly high gain antennas. In addition, since the proposed antenna design acts as a proof of concept, high gain can be easily achieved by using gain enhancement techniques like by integrating metamaterial unit cells in the radiating aperture [16] or by using dielectric loading [17].

The 1-dB gain bandwidth of the proposed mmWave 5G antenna is 47.6% indicating high pattern integrity across the entire operating band. Measured results were carried out in an anechoic chamber. Experimental setup for measuring radiation cuts is depicted in Fig. 6. Radiation patterns with high pattern integrity in the XY-plane (E-plane) are illustrated in Fig. 7. Since one metallic tapered arm of Vivaldi antenna is extended for providing proper grounding contact with the clamps of end-launch connector, radiation patterns are tilted by around 10–20 degrees. Front to back ratio of more than 15 dB is attained across the whole operating band. Disparity between simulated and measured radiation patterns might be due to alignment errors and adapters employed for pattern measurements.

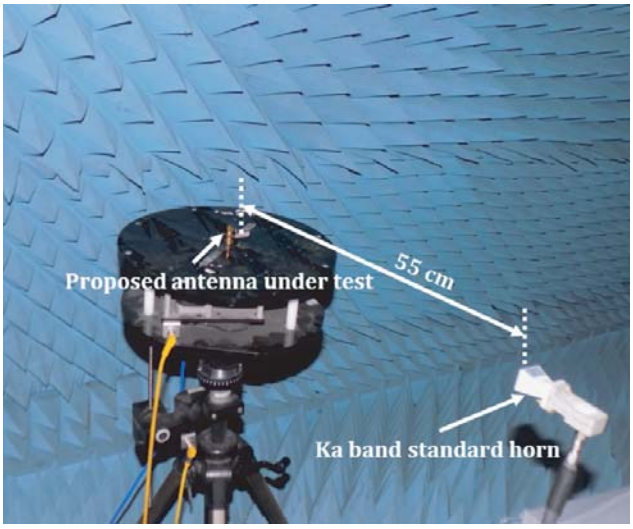

Figure 6. Experimental set-up for measuring radiation patterns of the proposed antenna.

2.3. Integrated Corner Bent 4G LTE and mmWAVE 5G Antenna MIMO Design

Co-designed 4G LTE and mmWave 5G antennas are integrated along the edge panel of smartphone for achieving orthogonal pattern diversity. Since polycarbonate based substrate is flexible, corner bending for decreasing effective radiating volume can be achieved easily.

The antennas were independently designed and integrated together. The rationale behind this design process is that the mesh size of the antenna model is related to the operating wavelength. When

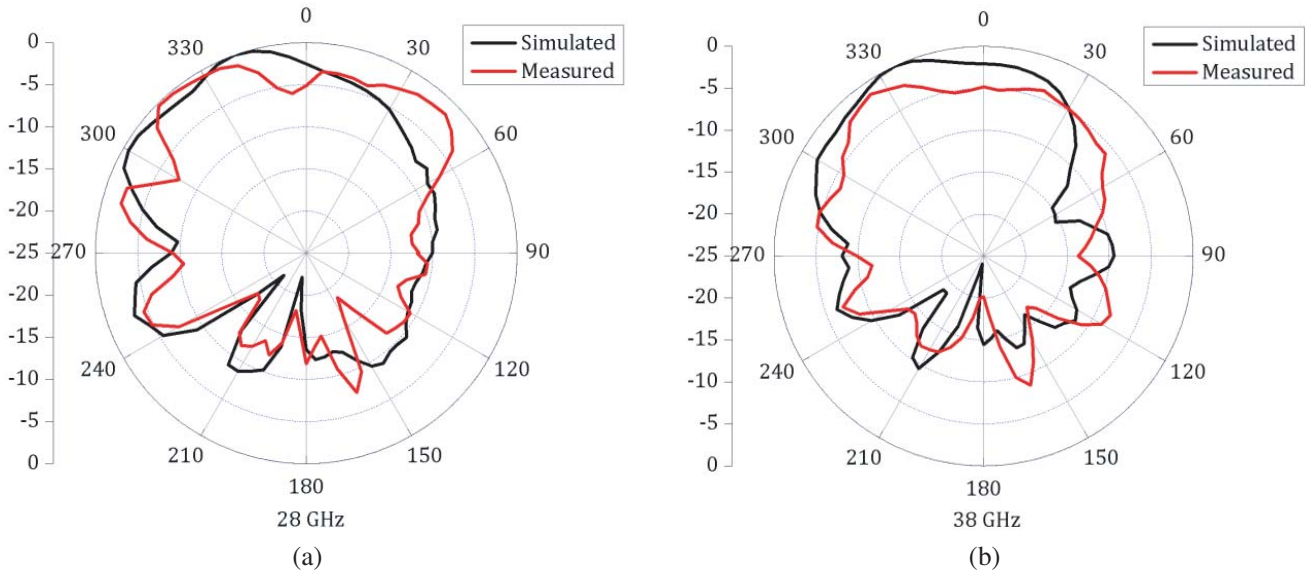

Figure 7. Radiation patterns in XY-plane for proposed mmWave 5G antenna.

the low frequency antenna model is simulated with high frequency settings, the computational time would increase due to fine mesh without any significant advantage in accuracy. On the other hand, if lower frequency settings are used to solve the high frequency antenna, the mesh size would be high leading to a compromise in the accuracy.

MIMO antenna configuration is obtained by inserting one co-designed 4G LTE and mmWave 5G antenna module on one edge panel of smartphone and the other antenna module on the opposite edge panel as illustrated in Fig. 8. The smartphone case is realized by fabricated Poly Lactic Acid (PLA) based three-dimensional housing. Since the physical footprint of each antenna module is minimal with dimensions of $6 \times 64.5 \times 0.5\,\text{mm}^3$, integration in the current commercially available smartphones can be achieved easily. Since the two antenna modules are electrically far from each other, antenna characteristics were not influenced by a large amount. Orthogonal pattern diversity is proposed for catering portrait and landscape modes of data usage. Table 1 illustrates the comparison of proposed integrated 4G LTE and mmWave 5G antenna architecture with other recently reported designs.

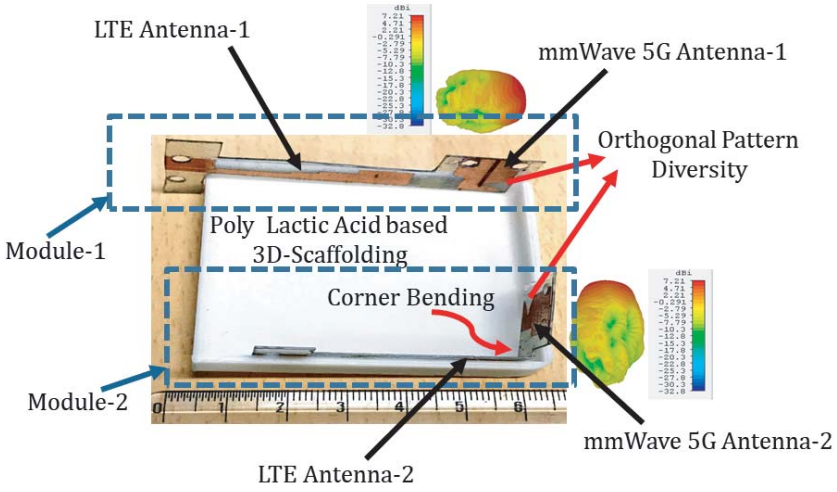

Figure 8. Co-designed 4G LTE and mmWave 5G MIMO antenna architecture with orthogonal pattern diversity integrated with three dimensional mobile phone case.

Table 1. Comparison of the proposed antenna architecture with other recently reported designs.

Figures of Merit	**Proposed Design**	**[3]**	**[4]**	**[5]**
4G LTE ANTENNA				
Area of single element	**$6 \times 44\,\text{mm}^2$**	$75 \times 8\,\text{mm}^2$	$14 \times 30\,\text{mm}^2$	$9 \times 30\,\text{mm}^2$
Fractional Bandwidth (BW)	**40% (−10 dB BW)**	31%-Low Band, 44%-High Band (−6 dB BW)	55% (−10 dB BW)	30% (−6 dB BW)
Operating LTE Bands	**LTE1900/2300/2500**	LTE700/1900/2300/2500	LTE1900/2300/2500	LTE1900/2300/2500
MIMO	**Yes**	No	Yes	Yes
Cost	**Low**	Relatively High	Relatively High	Relatively High
Corner Bent	**Yes**	No	Yes	No
Edge Panel Integration for future smartphones	**Feasible due to less antenna width**	Not feasible due to large physical footprint	Not feasible due to large antenna width	Not feasible due to large antenna width
mmWAVE 5G ANTENNA				
Area of antenna	**$6 \times 8\,\text{mm}^2$ (Single Element)**	$23 \times 7\,\text{mm}^2$ (1×4 array)	$17.5 \times 14\,\text{mm}^2$	$23.2 \times 8.3\,\text{mm}^2$ (2×4 array)
Impedance Bandwidth	**23–39 GHz**	25–30 GHz	25–38 GHz	26–28.4 GHz
Peak Realized Gain	**7.2 dB**	7 dB	10.5 dB	8.2 dB
1-dB Gain Bandwidth	**47.6%**	Not Available	28%	Not Available
Orthogonal Pattern Diversity	**Yes**	No	Yes	No
MIMO	**Yes**	No	Yes	No
Cost	**Low**	Relatively High	Relatively High	Relatively High
Corner Bent	**Yes**	No	Yes	No
Edge Panel Integration for future smartphones	**Feasible due to less antenna width**	Not feasible due to large physical footprint	Not feasible due to large antenna width	Not feasible due to large antenna width

3. CONCLUSION

Low cost substrate based co-designed 4G LTE and mmWave 5G antennas are proposed for future smartphones. The 4G LTE MIMO antenna module consists of two ACS-fed compact antennas with operational bandwidth ranging from 1.8 to 2.7 GHz. Gain of the antennas is reasonable for the available physical footprint. Orthogonal pattern diversity is achieved by designing two mmWave 5G Vivaldi antennas with small electrical size. The mmWave 5G antennas achieve wide impedance bandwidth with fractional bandwidth of 51.6%. The 1-dB gain bandwidth of each mmWave 5G antenna is around 47% indicating high pattern integrity across the entire operating band. Edge panel integration is achieved by inserting proposed MIMO antennas inside a three-dimensional PLA based fabricated prototype. Simulated and measured results validate that the proposed low cost substrate based antenna architecture is a suitable candidate for co-designed 4G LTE and mmWave 5G applications.

ACKNOWLEDGMENT

The authors would like to thank the Centre for Applied Research in Electronics (CARE) department of IIT Delhi for providing antenna testing facility.

REFERENCES

1. Hong, W., K. Baek, Y. Lee, Y. Kim, and S. Ko, "Study and prototyping of practically large-scale mmWave antenna systems for 5G cellular devices," *IEEE Communications Magazine*, Vol. 52, No. 9, 63–69, Sep. 2014.
2. Rappaport, T. S., et al., "Millimeter wave mobile communications for 5G cellular: It will work!," *IEEE Access*, Vol. 1, 335–349, 2013.
3. Kurvinen, J., H. Kähkönen, A. Lehtovuori, J. Ala-Laurinaho, and V. Viikari, "Co-designed mm-wave and LTE handset antennas," *IEEE Transactions on Antennas and Propagation*, Vol. 67, No. 3, 1545–1553, Mar. 2019.
4. Idrees Magray, M., G. S. Karthikeya, K. Muzaffar, and S. K. Koul, "Corner bent integrated design of 4G LTE and mmWave 5G antennas for mobile terminals," *Progress In Electromagnetics Research M*, Vol. 84, 167–175, 2019.
5. Hussain, R., A. T. Alreshaid, S. K. Podilchak, and M. S. Sharawi, "Compact 4G MIMO antenna integrated with a 5G array for current and future mobile handsets," *IET Microw. Antennas Propag.*, Vol. 11, No. 2, 271–279, Feb. 2017.
6. Idrees Magray, M., G. S. Karthikeya, K. Muzaffar, and S. K. Koul, "Compact co-design of conformal 4G LTE and mmWave 5G antennas for mobile terminals," *IETE Journal of Research*, 2019.
7. Sharawi, M. S., M. Ikram, and A. Shamim, "A two concentric slot loop based connected array MIMO antenna system for 4G/5G terminals," *IEEE Transactions on Antennas and Propagation*, Vol. 65, No. 12, 6679–6686, Dec. 2017.
8. Li, X., X. Shi, W. Hu, P. Fei, and J. Yu, "Compact triband ACS-fed monopole antenna employing open-ended slots for wireless communication," *IEEE Antennas and Wireless Propagation Letters*, Vol. 12, 388–391, 2013.
9. Rajkumar, R. and U. K. Kommuri, "A compact ACS-fed mirrored L-shaped monopole antenna with SRR loaded for multiband operation," *Progress In Electromagnetics Research C*, Vol. 64, 159–167, 2016.
10. Priyadarshi, R., M. P. Singh, H. Tripathi, and P. Sharma, "Design and performance analysis of Vivaldi antenna at very high frequency," *2017 Fourth International Conference on Image Information Processing (ICIIP)*, 1–4, Shimla, 2017.
11. Jarufe, C., et al., "Optimized corrugated tapered slot antenna for mm-Wave applications," *IEEE Transactions on Antennas and Propagation*, Vol. 66, No. 3, 1227–1235, Mar. 2018.
12. Dai, L. H., C. Tan, and Y. J. Zhou, "Ultrawideband low-profile and miniaturized spoof plasmonic Vivaldi antenna for base station," *Appl. Sci.*, Vol. 10, 2429, 2020.
13. Dixit, A. S. and S. Kumar, "A miniaturized antipodal Vivaldi antenna for 5G communication applications," *2020 7th International Conference on Signal Processing and Integrated Networks (SPIN)*, 800–803, Noida, India, 2020.
14. Dixit, A. S. and S. Kumar, "The enhanced gain and cost-effective antipodal Vivaldi antenna for 5G communication applications," *Microw. Opt. Technol. Lett.*, Vol. 62, 2365–2374, 2020.
15. Bhattacharjee, A., A. Bhawal, A. Karmakar, and A. Saha, "Design of an antipodal Vivaldi antenna with fractal-shaped dielectric slab for enhanced radiation characteristics," *Microw. Opt. Technol. Lett.*, Vol. 62, 2066–2074, 2020.
16. Muzaffar, K., M. I. Magray, G. S. Karthikeya, and S. K. Koul, "High gain broadband Vivaldi antenna for 5G applications," *2019 International Conference on Electromagnetics in Advanced Applications (ICEAA)*, 496–497, Granada, Spain, 2019.
17. Kota, K. and L. Shafai, "Gain and radiation pattern enhancement of balanced antipodal Vivaldi antenna," *Electronics Letters*, Vol. 47, No. 5, 303–304, Mar. 3, 2011.